idence for such stabilization has been seen in solution studies, and direct MHC class II–CD4 binding was not detected (*31*). These results and the data presented here instead suggest that the function of CD4 may be to "boost" or "trigger" the early phase of activation. Once that process is under way, CD4 seems to be excluded from the central core of the synapse, perhaps owing to the formation of some lattice-like structure by the remaining molecules.

References and Notes

1. A. Weiss and D. R. Littman, *Cell* **76**, 263 (1994).
2. R. König, L. Huang, R. N. Germain, *Nature* **356**, 796 (1992).
3. G. Cammarota *et al.*, *Nature* **356**, 799 (1992).
4. A. Kupfer and S. J. Singer, *J. Exp. Med.* **170**, 1697 (1989).
5. P. Marrack *et al.*, *J. Exp. Med.* **158**, 1077 (1983).
6. J. Hampl, Y-H. Chein, M. M. Davis, *Immunity* **7**, 379 (1997).
7. J. Madrenas, L. A. Chau, J. Smith, J. A. Bluestone, R. N. Germain, *J. Exp. Med.* **185**, 219 (1997).
8. J. M. Turner *et al.*, *Cell* **60**, 755 (1990).
9. D. B. Straus and A. Weiss, *Cell* **70**, 585 (1992).
10. M. M. Davis *et al.*, *Annu. Rev. Immunol.* **16**, 523 (1998).
11. C. A. Janeway Jr., *Annu. Rev. Immunol.* **10**, 645 (1992).
12. C. R. F. Monks, B. A. Freiberg, H. Kupfer, N. Sciaky, A. Kupfer, *Nature* **395**, 82 (1998).
13. A. Grakoui *et al.*, *Science* **285**, 221 (1999).
14. C. Wülfing, M. D. Sjaastad, M. M. Davis, *Proc. Natl. Acad. Sci. U.S.A.* **95**, 6302 (1998).
15. J. Kaye, S. Porcelli, J. Tite, B. Jones, C. A. Janeway Jr., *J. Exp. Med.* **158**, 836 (1983).
16. GFP fusion constructs were transfected into D10 by electroporation as described (*32*). After 1 to 2 weeks, these cultures were expanded into 24-well dishes, screened by flow cytometry, and sorted for GFP expression. Established clones were subjected to phenotypic analysis by staining for CD4, CD3ε, TCR, CD28, and CD25 as well as proliferation analysis against CA 134-147 and the variant peptides E8T and I5G.
17. Supplemental Web material is available at *Science* Online at www.sciencemag.org/feature/data/1050535.shl.
18. Clones were maintained by weekly restimulations as described (*15*), except that cultures were typically not supplemented with exogenous interleukin-2. Activation experiments were performed from 5 to 10 days after the stimulation culture. CH27 is a B cell lymphoma that expresses IA^k, B7-1, and B7-2. Experiments were done at 37°C as described (*14*).
19. GFP intensity data were corrected both for background intensity and for photobleaching. Background level was measured by imaging a dish in the absence of cells. This background level was subtracted from intensity data to obtain background-subtracted data sets. For bleaching, a nonreactive cell was analyzed for surface intensity over time, and the intensity over time was fitted to an exponential decay curve ($I_t = I_0 10^{kt}$, where k is the decay constant, t is the number of times the fluorophore was illuminated at a constant rate, and I_t and I_0 are the initial intensities and intensities at time t). The decay constant k was used to calculate a correction factor ($1/10^{kt}$) for each time point in the experimental data sets. Typical decay constants were ~0.01, giving half-lives of about 30 illuminations. Typical experiments involved about 60 to 80 illuminations.
20. Intensities from 340- and 380-nm excitations of Fura-2 were used to make a ratio image. Background calcium levels were obtained from at least five frames before activation and were similar to nonreactive cells from other portions of the field. Increases of 30% above background were found to be well above random fluctuations, and the onset of agonist-driven reactions typically was characterized by at least a 100% increase in a single 15-s time period. Individual cells were analyzed for maximal pixel intensities along the leading edge of cells by a line-scan function. All collected z planes were analyzed and compared to the average from three intensity line scans (taken at different z planes) around the circumference of the cell of interest. Background- and bleach-corrected data were used for all analyses. Rectangular x-y regions encompassing the estimated interface were determined from the differential interference contrast (DIC) image, and z stacks encompassing these regions were used for the interface projections. Max Intensity Projections were used (Metamorph, Universal Imaging, PA).
21. C. Wülfing and M. M. Davis, unpublished observations.
22. _____, *Science* **282**, 2266 (1998).
23. A. Viola, S. Schroeder, Y. Sakakibara, A. Lanzavecchia, *Science* **283**, 680 (1999).
24. S. Caplan, S. Zeliger, L. Wang, M. Baniyash, *Proc. Natl. Acad. Sci. U.S.A.* **92**, 4768 (1995).
25. M. M. Rozdzial, B. Malissen, T. H. Finkel, *Immunity* **3**, 623 (1995).
26. J. R. Cochran, T. O. Cameron, L. J. Stern, *Immunity* **12,** 241 (2000).
27. J. J. Boniface *et al.*, *Immunity* **9,** 459 (1998).
28. M. D. Bootman, M. J. Berridge, P. Lipp, *Cell* **91,** 367 (1998).
29. Z. Reich *et al.*, *Nature* **387**, 617 (1997).
30. P. A. Negulescu, N. Shastri, M. D. Calahan, *Proc. Natl. Acad. Sci. U.S.A.* **91**, 2873 (1994).
31. N. Barclay and P. A. van der Merwe, unpublished observations.
32. J. Kaye and S. M. Hedrick, *Nature* **336**, 580 (1988).
33. A. Viola and A. Lanzavecchia, *Science* **273**, 104 (1996).
34. M. F. Krummel, M. D. Sjaastad, C. Wülfing, M. M. Davis, data not shown.

35. We are grateful to J. Huppa, C. Sumen, and L. Richie for critical comments and advice. We thank C. Terhorst and J. Parnes for supplying the cDNAs for CD3ζ and CD4, respectively. We also thank the Stanford Shared FACS Facility for assistance in cell sorting. Supported by a postdoctoral award from the National Institutes of Health (M.F.K.) and by the Howard Hughes Medical Institute and NIH.

20 March 2000; accepted 13 July 2000

Treatment of Murine Colitis by *Lactococcus lactis* Secreting Interleukin-10

Lothar Steidler,[1]*† Wolfgang Hans,[1]† Lieven Schotte,[1] Sabine Neirynck,[1] Florian Obermeier,[2] Werner Falk,[2] Walter Fiers,[1] Erik Remaut[1]

The cytokine interleukin-10 (IL-10) has shown promise in clinical trials for treatment of inflammatory bowel disease (IBD). Using two mouse models, we show that the therapeutic dose of IL-10 can be reduced by localized delivery of a bacterium genetically engineered to secrete the cytokine. Intragastric administration of IL-10–secreting *Lactococcus lactis* caused a 50% reduction in colitis in mice treated with dextran sulfate sodium and prevented the onset of colitis in IL-$10^{-/-}$ mice. This approach may lead to better methods for cost-effective and long-term management of IBD in humans.

Inflammatory bowel disease (IBD), including Crohn's disease and ulcerative colitis, is a significant public health problem in Western societies, affecting 1 in 1000 individuals, yet its etiology remains poorly understood. IBD is characterized clinically by chronic inflammation in the large and/or small intestine, the symptoms of which include diarrhea, abdominal pain, weight loss, and nausea. Death can result, in extreme cases, from malnutrition, dehydration, and anemia. IBD is thought to arise from interacting genetic and environmental factors (*1*) and may involve abnormal T cell responses to commensal microflora (*2–4*). Biologically based therapies such as antibodies to tumor necrosis factor (TNF), which is a strong proinflammatory mediator (*5–7*), and recombinant IL-10 (*8*) can ameliorate the disorder.

Because IL-10 has a central role in downregulating inflammatory cascades (*9*) and matrix metalloproteinases (*10*), it is a likely candidate for use in therapeutic intervention. In this study we have tested a new method of delivering IL-10: in situ synthesis by genetically engineered bacteria (*Lactococcus lactis*), in two mouse models of the disease, one involving treatment of chronic colitis induced by 5% dextran sulfate sodium (DSS) (*11*) and one involving prevention of colitis that spontaneously develops in IL-$10^{-/-}$mice (*12*). We show that this approach, which depends on in vivo synthesis of IL-10, requires much lower doses than systemic treatment. Neither mouse model mimics all aspects of human IBD, but such models are essential for development of new therapeutic approaches to IBD (*13–20*).

L. lactis is a nonpathogenic, noninvasive, noncolonizing Gram-positive bacterium, mainly used to produce fermented foods. We previously constructed recombinant *L. lactis* strains for production and in vivo delivery of cytokines

[1]Department of Molecular Biology, Ghent University and Flanders Interuniversity Institute for Biotechnology, K. L. Ledeganckstraat 35, 9000 Gent, Belgium. [2]Department of Internal Medicine I, University of Regensburg, Franz-Josef-Strauss-Allee 11, 93042 Regensburg, Germany.

*To whom correspondence should be addressed. E-mail: lothar.steidler@dmb.rug.ac.be

†These authors contributed equally to this work.

(*21*–*23*). We have now engineered an *L. lactis* strain (*LL-mIL10*) for secretion of biologically active murine IL-10 (mIL-10) (Fig. 1) (*24*, *25*).

To evaluate the efficacy of the new therapeutic concept, we applied daily intragastric inocula (*24*) of 2×10^7 *LL-mIL10* or control *L. lactis* (*25*) to mice in which chronic colitis had been induced by four cycles of administration of DSS in the drinking water for 7 days, alternating with 10-day periods of recovery (*11*, *26*). Treatment was arbitrarily initiated at day 21 after the fourth DSS administration. The predominant epithelial damage was loss of goblet cells and crypts (Fig. 2A) (*25*). A lymphocytic infiltrate was largely restricted to the thickened mucosa of the middle and distal colon; submucosa was affected in about 10% of mice. Inflammation typically persisted for at least 3 months. The chronic phase of inflammation showed complete regeneration of the intestinal epithelial lining. The range of inflammation is shown in histological images from the distal colon (Fig. 2A) and middle colon (*25*).

Histological scores were devised to allow quantification of histological changes (Fig. 3A). Scores from individual mice ($n = 10$) after treatment with different *L. lactis* strains were recorded after blinded interpretation of sections from the distal colon (*26*). Untreated healthy mice had a histological score of 1, whereas mice with the induced chronic colitis and mock-treated control mice had a score of ~5. Mice treated for 14 days with *LL-mIL10* given by gastric catheter, followed by 14 days of recovery, had an average histological score of ~3. This represents a nearly 50% decrease ($P = 0.0151$) in pathological symptoms, a more pronounced improvement than that obtained with standard systemic treatment with TNF monoclonal antibodies (mAbs), which leads to a 30 to 40% decrease in inflammation (*26*). In the *LL-mIL10*–treated group, colons of 4 of 10 mice had the histological characteristics of healthy mice, and 4 showed minor patchy remnants of inflammation (*25*); in 2 mice, larger areas remained affected. No further improvement was observed when *LL-mIL10* treatment was extended to 4 weeks; when the daily inoculum was 10^9 bacteria rather than 2×10^7, the improvement in pathology was less pronounced (*27*). Mice with DSS-induced colitis occasionally developed adenomas (*25*), corresponding to development in humans of adenocarcinoma often seen associated with ulcerative colitis. By contrast, no adenomas were seen in mice treated for 14 days with *LL-mIL10*.

We also evaluated the ability of *LL-mIL10* to prevent the onset of colitis in IL-$10^{-/-}$ mice, which spontaneously develop colitis at age 3 to 8 weeks (*12*). This progressive disease is characterized by multifocal inflammatory cell infiltrates (mononuclear cells and neutrophils), moderate epithelial hyperplasia, and slight mucin depletion from goblet cells. Other work has shown that treatment of 3-week-old IL-$10^{-/-}$ mice with recombinant mIL-10, interferon-γ mAbs, or IL-12 mAbs prevents the onset of colitis (*16*, *28*). In our studies, the untreated IL-$10^{-/-}$ mice showed less severe inflammation than that observed by other workers (*16*, *29*). We treated 3-week-old mice ($n = 5$) by daily intragastric inocula of 2×10^7 or 10^9 *LL-mIL10* or control *L. lactis* as for the DSS-induced colitis model (Fig. 2) (*25*). Untreated mice had a mean histological score of ~4.5, whereas the *LL-mIL10*–treated group had a mean score of 1.5, which only slightly exceeds values reported for control mice (*16*) (Fig. 3B). In contrast to results with DSS-induced colitis, treatment effi-

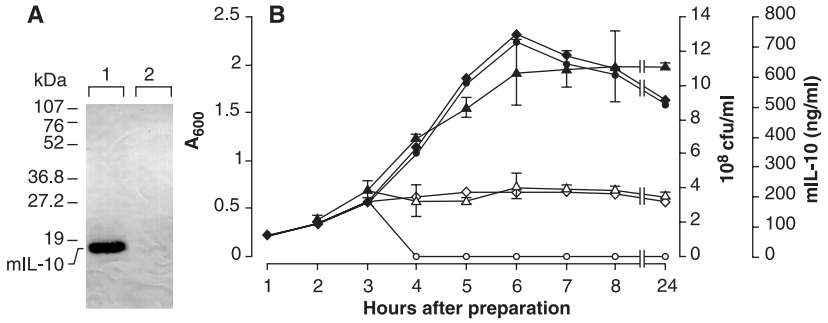

Fig. 1. mIL-10 synthesis by *LL-mIL10*. (**A**) Western blot analysis of culture supernatant proteins from the mIL-10 producer strain *LL-mIL10* (lane 1) and the vector control *LL-TREX1* (lane 2) (*24*, *25*), revealed with anti–mIL-10 (Pepro Tech EC, London, UK). The position of mIL-10 is indicated. The concentration of mIL-10 in the culture supernatant was 3 μg/ml, as determined by enzyme-linked immunosorbent assay. The biological activity in the culture supernatant was estimated at 10,000 U/ml in a cell proliferation bioassay with the IL-10–dependent mast cell line MC/9 (*33*). When compared with a standard of known activity (BioSource International, Camarillo, California), the recombinant mIL-10 from the *LL-mIL10* culture supernatant revealed full specific biological activity. The NH_2-terminus of this protein was determined, by automated Edman degradation, to be Gln-Tyr-Ser-Arg-Glu, which is identical to that of native mIL-10. (**B**) A_{600} (◆), colony-forming units (CFU) (●), and mIL-10 concentration (▲) for an *LL-mIL10* culture, prepared as for the inoculation of mice with 2×10^7 bacteria (*24*). Open symbols are for corresponding profiles of an identical culture that was UV-irradiated 3 hours after preparation. UV-irradiation immediately blocked the accumulation of mIL-10 in the culture supernatant and reduced the CFU count by 6 logarithmic units. No lysis was observed (*25*).

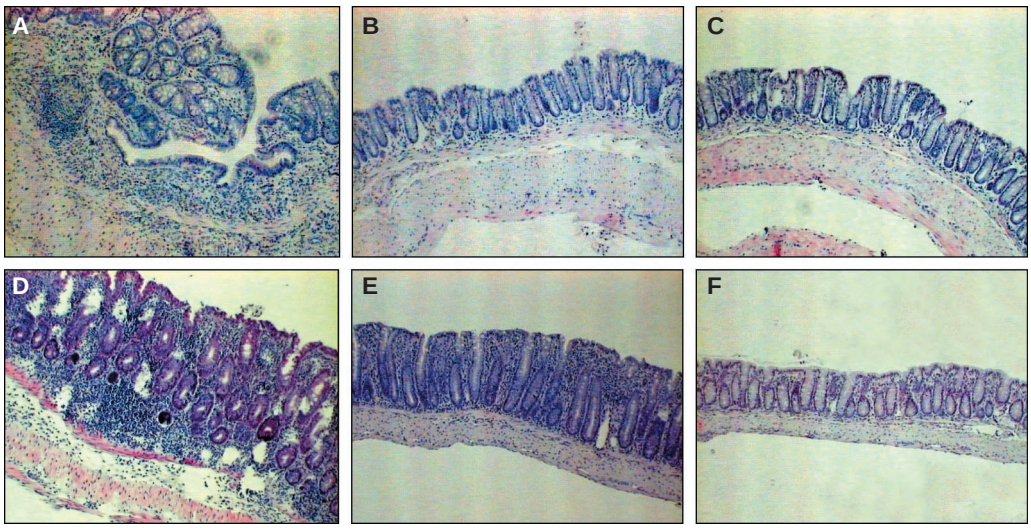

Fig. 2. Intestinal histology of murine colitis models. Images represent sections of the distal colon (magnification, ×100). Hematoxylin and eosin staining. (**A** to **C**) Inflammation in the DSS-induced colitis model, established in female Balb/c mice. Lymphocytic infiltrate and disturbance of tissue architecture was observed in untreated mice (A). After treatment by 14 daily intragastric inocula of 2×10^7 *LL-mIL10* per mouse followed by 14 days of recovery, the lymphocytic infiltrate was reduced and the tissue architecture was restored (B). Healthy control mice (C). (**D** to **F**) Images from 7-week-old female 129Sv/Ev IL-$10^{-/-}$ mice. Lymphocytic infiltrate is apparent in untreated mice (D) and mice treated for 4 weeks by daily intragastric inocula of 2×10^7 *LL-TREX1* (E) but not in mice treated for 4 weeks by daily intragastric inocula of 2×10^7 *LL-mIL10* (F).

cacy was the same for both inocula concentrations (*27*).

We confirmed that the therapeutic effect was due to mIL-10 synthesized de novo by *LL-mIL10* rather than to residual amounts of mIL-10 in the inocula. Indeed, because of the culture conditions used, a minor amount of mIL-10 (40 ng) (Fig. 1B) was present in the supernatant of the inoculum. The fate of this residual mIL-10 is likely acid denaturation, followed by breakdown in the stomach and duodenum (*25*). Diseased mice (DSS-induced colitis) treated for 2 or 4 weeks with ultraviolet (UV)-killed *LL-mIL10* cultures (Fig. 1B) (*25*) showed no difference in colon histology compared with control mice positive for colitis (Fig. 3A). This result indicates that the therapeutic effects require physiologically active *LL-mIL10*.

We also investigated the synthesis of recombinant mIL-10 by *LL-mIL10* in the intestine of IL-10$^{-/-}$ mice, which cannot themselves synthesize mIL-10. After administration of a total of 2.4×10^{10} *LL-mIL10* (as serial inocula), we detected 7×10^8 *LL-mIL10* and 7 ng of mIL-10 in the colon (*25*). Hence, these bacteria can actively produce mIL-10 in the colon, albeit at a lower yield than that observed in culture. This result agrees well with recent findings that *L. lactis* is metabolically active in all compartments of the intestinal tract (*30*). Although *LL-mIL10* organisms were present in other areas of the gastrointestinal tract (cecum, ileum, jejunum, and stomach), mIL-10 was not detectable there. Perhaps mIL-10 reached detectable levels only in the colon because in this part of the intestine the protein is not degraded, and the contents move slowly enough to allow its accumulation.

We compared the performance of *LL-mIL10*–mediated mIL-10 delivery with that of standard anti-inflammatory methods: systemic treatment (five daily intraperitoneal injections) with recombinant mIL-10, IL-12 mAbs (*31*), or dexamethasone. All therapies decreased inflammation in DSS-induced colitis by ~50% (Fig. 3A). Our method, however, required a much lower amount of mIL-10. We estimated that 14 daily inoculations of 2×10^7 *LL-mIL10* delivered ~1 U of mIL-10 per mouse (*25*), i.e., an amount that is several orders of magnitudes lower than the optimized total amount of intraperitoneally injected mIL-10 (1.25×10^4 U per mouse).

We propose two possible routes by which mIL-10 might reach its therapeutic target. The lactococci may produce mIL-10 in the lumen, and the protein may diffuse to responsive cells in the epithelium or the lamina propria. Alternatively, the lactococci may be taken up by M cells (bacterial size and shape would allow this), and the major part of the effect may be due to recombinant mIL-10 production in situ in intestinal lymphoid tissue. Both routes may involve paracellular transport mechanisms that are enhanced in inflammation. After transport, mIL-10 may directly down-regulate inflammation. Alternatively, autocrine mIL-10 secretion by lymphoid cells, as shown by transfer of Tr1 cells (*32*), epithelial cells, or both, may be induced and may enhance repair.

In summary, the method described here—cost-effective localized delivery of a therapeutic agent that is actively synthesized in situ by food-grade bacteria—may have potential clinical applications for treatment of IBD, particularly as an alternative to systemic treatment. In principle, the method may also be useful for intestinal delivery of other protein therapeutics that are unstable or difficult to produce in large quantities.

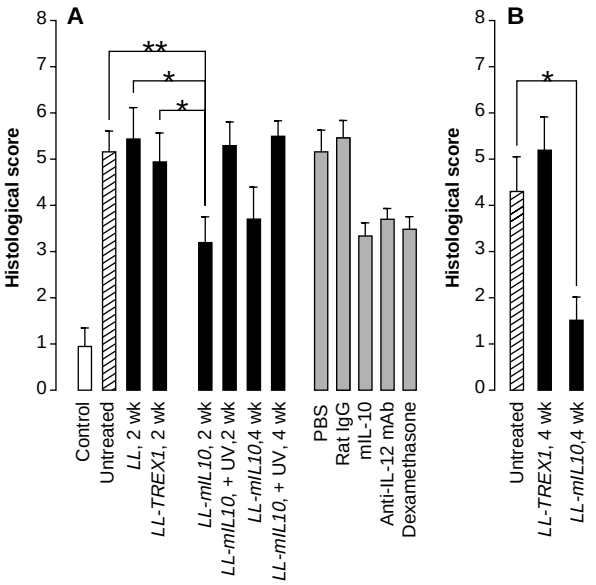

Fig. 3. Statistical evaluation of colon histology. Colon sections were randomly numbered and interpreted in a blinded manner. Scores from individual mice were subsequently decoded, and regrouped numbers were analyzed statistically. Bars represent the mean ± SEM. *$P < 0.025$; **$P = 0.0151$. (**A**) Histological scores (sum of epithelial damage and lymphoid infiltrate, both ranging from 0 to 4) for the distal colon of groups ($n = 10$) of control female Balb/c mice (white bar) and of female Balb/c mice with DSS-induced colitis that were untreated (hatched bar), treated with the indicated *L. lactis* cultures (black bars), or treated with five daily intraperitoneal injections of the compounds indicated (gray bars) (mIL-10: 5 μg per mouse per day; anti–IL-12: 1 mg per mouse per day; dexamethasone: 5 μg per mouse per day; rat IgG: 5 μg per mouse per day). Mice treated daily for 2 or 4 weeks (wk) with 2×10^7 mIL-10–producing *LL-mIL10* showed significantly reduced inflammation when compared with untreated or control-treated (*LL* or *LL-TREX1*) mice. This effect was not observed when *LL-mIL10* cultures were UV-killed (+UV). (**B**) Histological scores (sum of the degrees of inflammation in the proximal, middle, and distal colon, all ranging between 0 and 4) obtained after blinded interpretation of groups ($n = 5$) of 7-week-old untreated (hatched bar), *LL-TREX1*–treated, or *LL-mIL10*–treated female 129 Sv/Ev IL-10$^{-/-}$ mice (black bars). *LL-mIL10*–treated mice showed significantly less inflammation than untreated mice.

References and Notes

1. R. B. Sartor, *Am. J. Gastroenterol.* **92,** 5S (1997).
2. H. C. Rath *et al.*, *J. Clin. Invest.* **98,** 945 (1996).
3. R. K. Sellon *et al.*, *Infect. Immun.* **66,** 5224 (1998).
4. T. T. MacDonald, G. Monteleone, S. L. Pender, *Scand. J. Immunol.* **51,** 2 (2000).
5. S. R. Targan *et al.*, *N. Engl. J. Med.* **337**, 1029 (1997).
6. H. M. van Dullemen *et al.*, *Gastroenterology* **109**, 129 (1995).
7. G. D'Haens *et al.*, *Gastroenterology* **116**, 1029 (1999).
8. S. J. van Deventer, C. O. Elson, R. N. Fedorak, *Gastroenterology* **113**, 383 (1997).
9. P. Stordeur and M. Goldman, *Int. Rev. Immunol.* **16**, 501 (1998).
10. S. L. Pender *et al.*, *Gastroenterology* **115**, 573 (1998).
11. I. Okayasu *et al.*, *Gastroenterology* **98**, 694 (1990).
12. R. Kuhn, J. Lohler, D. Rennick, K. Rajewsky, W. Muller, *Cell* **75**, 263 (1993).
13. M. F. Neurath, I. J. Fuss, B. L. Kelsall, E. Stuber, W. Strober, *J. Exp. Med.* **182**, 1281 (1995).
14. R. O. Ehrhardt, B. R. Ludviksson, B. Gray, M. F. Neurath, W. Strober, *J. Immunol.* **158**, 566 (1997).
15. M. Boirivant, I. J. Fuss, A. Chu, W. Strober, *J. Exp. Med.* **188**, 1929 (1998).
16. D. J. Berg *et al.*, *J. Clin. Invest.* **98**, 1010 (1996).
17. D. Picarella *et al.*, *J. Immunol.* **158**, 2099 (1997).
18. D. K. Podolsky *et al.*, *J. Clin. Invest.* **92**, 372 (1993).
19. K. L. Madsen, J. S. Doyle, L. D. Jewell, M. M. Tavernini, R. N. Fedorak, *Gastroenterology* **116**, 1107 (1999).
20. J. K. Collins *et al.*, *Gastroenterology* **116**, G2981 (1999).
21. L. Steidler *et al.*, *Appl. Environ. Microbiol.* **61**, 1627 (1995).
22. L. Steidler, W. Fiers, E. Remaut, in *Current Advances in Genetics, Metabolism and Application of Lactic Acid Bacteria*, F. Bozoglu and B. Ray, Eds. (NATO ASI Series H, Springer, Berlin, 1996), vol. 98, pp. 63–79.
23. L. Steidler *et al.*, *Infect. Immun.* **66**, 3183 (1998).
24. Standard media were M17 (Difco Laboratories, Detroit, MI) and M9 [6 g of Na_2HPO_4, 3 g of KH_2PO_4, 1 g of NH_4Cl, 0.5 g of NaCl, 0.12 g of $MgSO_4$, 0.01 g of $CaCl_2$, and 5 g of Casitone (Difco Laboratories) per liter], or GM17 and GM9 when supplemented with 0.5% glucose. BM9 means GM9 buffered with 50 mM CO_3^{2-}. During growth in GM17 or GM9, *L. lactis* produces lactate, so that the acidity of the culture drops to pH 5.5. Probably because of its known acid sensitivity, no recombinant mIL-10 was detected in the *LL-mIL10* culture supernatants. We tested a series of CO_3^{2-}-buffered BM9 cultures, with the pH ranging from 7 to 9.5. For optimal mIL-10 protein synthesis, saturated cultures that had grown overnight in GM17 were diluted 1:100 in fresh GM17 and grown for 3 hours. Bacteria were collected by centrifugation, were resuspended in an equal volume of BM9 buffered to pH 8.5, and were grown for 5 hours more, at which point the pH was ~7.0. For all intragastric inoculations, BM9 was used at an initial pH of 8.5. Stock suspensions of all strains were stored at −20°C in 50% glycerol-GM17. Precultures were grown daily by diluting stock suspensions 200-fold in fresh GM17. These cultures grow to saturation within 16 hours when incubated at 30°C. Bacterial cells either were collected at this stage and concentrated 10-fold in BM9 medium (given as a 100-μl inoculum of 10^9 bacteria) or were diluted 25-fold in BM9 and grown for 3 hours at 30°C (given as a 200-μl inoculum of 2×10^7 bacteria). Earlier studies had shown that bacteria from both types of suspensions secrete similar quantities of recombinant proteins.

25. For further details, see *Science* Online at www.sciencemag.org/feature/data/1047997.shl.
26. G. Kojouharoff *et al.*, *Clin. Exp. Immunol.* **107**, 353 (1997).
27. L. Steidler *et al.*, data not shown.
28. D. M. Rennick, M. M. Fort, N. J. Davidson, *J. Leukocyte Biol.* **61**, 389 (1997).
29. Mice were housed in ventilated cages in which incoming and outgoing air was filtered over a high-efficiency particulate air filter. All manipulations were performed inside a class II biosafety hood. This "clean" housing may account for the lower degree of intestinal inflammation in our mice than that previously reported in the literature.
30. G. Corthier, C. Delorme, S. D. Ehrlich, P. Renault, *Appl. Environ. Microbiol.* **64**, 2721 (1998).
31. M. Wysocka *et al.*, *Eur. J. Immunol.* **25**, 672 (1995).
32. H. Groux *et al.*, *Nature* **389**, 737 (1997).
33. L. Thompson-Snipes *et al.*, *J. Exp. Med.* **173**, 507 (1991).
34. We thank I. Bruggeman, H. Devlies, K. Pollinger, and K. Van Laer for technical assistance; J. Wells for pTREX1; T. Velu for mIL-10 cDNA; K. Madsen for 129Sv/Ev IL-10$^{-/-}$ mice; G. Trinchieri for anti–IL-12–producing C17.8 hybridoma cells; J. Van Snick for MC/9 cells; M. Praet for automated tissue processing; and C. Cuvelier, K. Madsen, and P. Vandenabeele for helpful discussion and critically reading the manuscript. L.S. is a fellow with the Vlaams Instituut voor de Bevordering van het Wetenschappelijk-technologisch Onderzoek in de Industrie. Supported by grants 1.5567.98N and G005097 of the Fonds voor Wetenschappelijk Onderzoek–Vlaanderen.

16 December 1999; accepted 10 July 2000

Whistle Matching in Wild Bottlenose Dolphins (*Tursiops truncatus*)

Vincent M. Janik

Dolphin communication is suspected to be complex, on the basis of their call repertoires, cognitive abilities, and ability to modify signals through vocal learning. Because of the difficulties involved in observing and recording individual cetaceans, very little is known about how they use their calls. This report shows that wild, unrestrained bottlenose dolphins use their learned whistles in matching interactions, in which an individual responds to a whistle of a conspecific by emitting the same whistle type. Vocal matching occurred over distances of up to 580 meters and is indicative of animals addressing each other individually.

Bottlenose dolphins show many cognitive and communicative skills that are rare among animals. They are capable not only of generalizing rules, developing abstract concepts and syntactic understanding in an artificial communication system (*1*), but also of vocal learning, i.e., the ability to modify the structure of a vocal signal as a result of experience with those of other individuals (*2*). Although extensive studies in nonhuman primates have not been able to present convincing evidence for vocal learning, this prerequisite for the evolution of spoken language has been demonstrated with much less research effort in bottlenose dolphins (*2*). Dolphins are capable of imitating new sounds accurately at their first attempt, and they keep this ability throughout their life (*3*). Vocal learning is also an important factor in the ontogeny of an individually distinctive signature whistle that each individual develops in the first few months of its life (*4*). Studies on captive individuals have shown that signature whistles are primarily used if animals are out of sight of each other, and they are therefore thought to function in group cohesion and individual recognition (*5*–*7*). However, because bottlenose dolphins are capable of vocal learning, individual signature whistles can be found in the repertoire of more than one individual in captive dolphins (*6*, *8*).

I investigated whether such shared whistles occur in matching whistle interactions between wild dolphins, a phenomenon indicative of their use in addressing specific individuals. Matching interactions were defined as an occurrence in which two whistles of the same type produced by separate individuals occurred within 3 s of each other.

There is often a clear effect of observer presence on dolphin behavior when methods such as tagging or boat pursuits are applied (*6*, *9*). I used a noninvasive passive acoustic localization technique (*10*) to locate calling bottlenose dolphins (*11*). This method uses the differences in the time of arrival of the same sound at different widely spaced hydrophones. Signals from different recording channels were cross-correlated to determine the difference in the time of arrival of a sound at the two corresponding hydrophones. The time-of-arrival comparisons of three pairs of hydrophones then result in three hyperbolas of possible sound source locations. These hyperbolas intersect at the true location of the whistling dolphin. This analysis was conducted with SIGNAL software (Engineering Design, Belmont, Massachusetts). Recordings were conducted in the Kessock Channel of the Moray Firth, Scotland. All data were acquired from the shore, so that no boats or humans were present around the animals.

Vocal interactions between individuals were identified by comparing the distance of the source locations of two successive whistles (minus twice the maximum localization error of 13 m) with the distance that a bottlenose dolphin could travel at its maximum reported swimming speed of 7.5 m/s (*12*) in the interwhistle interval. If the distance between two whistle sources could not have been covered by one individual in the time interval between those whistles, they must have been produced by different individuals.

Five naïve human observers were used to rate the similarity of each whistle interaction using only the extracted contours (*13*) of the whistles; this method is more reliable than computer-based methods that have been used in dolphin whistle studies (*14*). They were allowed to rate whistle similarity on a scale from 1 (=dissimilar) to 5 (=similar). The scores of the different observers were significantly similar (Kappa = 0.34, $z = 16.9$, $P < 0.00001$). Only whistle pairs that reached an average score of more than 3.0 were considered to be matching interactions (*15*).

In a total recording time of 258 min and 43 s from seven different days in July and August 1994 and 1995, a total of 1719 whistles was recorded. These recordings were made with an average of 10 animals present in the channel (quartiles: 7, 10, and 15). Independent counts conducted by a second observer from a higher observation point using binoculars showed that these counts were highly accurate. I could not identify individuals in this study, but a photo-identification study showed that at least 14 different individuals were using this area on a regular basis and that occasionally groups of more than 20 animals were present (*16*). Nine hundred ninety-one of the recorded whistles had a sufficient signal-to-noise ratio on all hydrophones for their source location to be determined. In this sample, 176 whistle interactions were found, of which 39 were classified as matching interactions (Fig. 1). In both matching and nonmatching interactions, 80% of the interwhistle interval was less than 1 s. The mean distance between matching individuals was 179 m (standard error: 22.8 m); the maximum was 579 m. Distances between animals in matching interactions were significantly smaller than those of animals in nonmatching interactions (Kolmogorov-Smirnov Two-Sample Test, two-tailed, $D = 0.291$, $P < 0.025$) (Fig. 2). A randomization test (*17*) showed that this number of matching interactions was signifi-

School of Biology, University of St. Andrews, Bute Building, Fife KY16 9TS, UK, and Lighthouse Field Station, Aberdeen University, Cromarty, Ross-shire IV11 8YJ, UK. Present address: Woods Hole Oceanographic Institution, Biology Department, Woods Hole, MA 02543, USA.